THE FASEB JOURNAL • RESEARCH • www.fasebj.org

Integrin α11 in pancreatic stellate cells regulates tumor stroma interaction in pancreatic cancer

Jonas Schnittert,* Ruchi Bansal,* Deby F. Mardhian,* Joop van Baarlen,† Arne Östman,‡ and Jai Prakash*,‡,1

*Department of Biomaterials, Science, and Technology, TechMed Centre, Targeted Therapeutics Section, Faculty of Science and Technology, University of Twente, Enschede, The Netherlands; †Laboratory Pathology East Netherlands (LabPON), Hengelo, The Netherlands; and ‡Department of Oncology-Pathology, Cancer Centre Karolinska, Karolinska Institutet, Stockholm, Sweden

ABSTRACT: Pancreatic ductal adenocarcinoma (PDAC) is the deadliest tumor due to its highly abundant tumor stroma. Pancreatic stellate cells (PSCs) are considered precursor cells of cancer-associated fibroblasts (CAFs), which induce tumor progression, invasion, and metastasis. In this study, we investigated the role of integrin subunit α (ITGA) 11, the receptor for collagen type I, in tumor stroma interaction. Clinical sample analysis showed that ITGA11 was overexpressed by CAFs in PDAC stroma, as shown with colocalization immunostaining with α−smooth muscle actin. In contrast, there was no expression in healthy pancreas. Public transcriptomic data confirmed a reduced expression of ITGA11 in healthy pancreas and adjacent nontumoral tissues compared with human tumor tissues. Primary human PSCs (hPSCs) activated with either TGF-β or pancreatic cancer cell (PANC-1)–conditioned medium (CM) resulted in the significant up-regulation of ITGA11 and various CAF markers. Furthermore, short hairpin RNA (shRNA)-mediated stable ITGA11 knockdown (shITGA11) in hPSCs significantly inhibited TGF-β– and PANC-1 CM−mediated activation at both gene and protein levels of extracellular matrix, cytokines, and adhesion molecules. Additionally, shITGA11 hPSCs had a reduced migration and contractility compared with shRNA control (shCTR) PSCs. Furthermore, we investigated the effect of ITGA11 on the paracrine effects of hPSCs. Interestingly, the CM from shITGA11 hPSCs, activated with either TGF-β or PANC-1 CM, caused tumor cells to migrate and invade lesser compared with their counterpart, activated shCTR PSCs. In summary, this study presents ITGA11 as an interesting stromal therapeutic target that plays a crucial role in the regulation of the differentiation of PSCs into CAFs and paracrine effects.—Schnittert, J., Bansal, R., Mardhian, D. F., van Baarlen, J., Östman, A., Prakash, J. Integrin α11 in pancreatic stellate cells regulates tumor stroma interaction in pancreatic cancer. FASEB J. 33, 6609–6621 (2019). www.fasebj.org

KEY WORDS: tumor microenvironment · cancer-associated fibroblasts · transforming growth factor β · cell migration · metastasis

Pancreatic ductal adenocarcinoma (PDAC) is one of the most devastating diseases in our society, with a 5-yr survival rate of only 8% (1). Due to the advanced stage of the disease, a surgical resection of the tumor is not feasible in most of the patients with PDAC. Therefore, radiotherapy or cytotoxic chemotherapy are the gold standards of treatment, but these treatments are not effective for PDAC, which results in a survival benefit of only a few months (2, 3). One of the biologic features that contributes to the high drug resistance, progression, invasion, and metastasis of PDAC is the abundant desmoplastic reaction, also known as the tumor stroma (4). The pancreatic tumor stroma can take up to 90% of the entire tumor mass, and its main cellular components are cancer-associated fibroblasts (CAFs), which support PDAC progression by producing extracellular matrix (ECM) proteins and secreting various cytokines and growth factors, which stimulate tumor growth, angiogenesis, invasion, and metastasis (5–7).

Studies have shown antitumoral effects of tumor stroma modulation in pancreatic tumor (8, 9), whereas on the contrary, complete genetic depletion of the

ABBREVIATIONS: α-SMA, α–smooth muscle actin; CAF, cancer-associated fibroblast; CM, conditioned medium; Col1a1, collagen type I α1 chain; CXCR-4, C-X-C chemokine receptor type 4; ECM, extracellular matrix; FBS, fetal bovine serum; hPSC, human pancreatic stellate cell; HRP, horseradish peroxidase; IDI1, isopentenyl-diphosphate Δ-isomerase 1; INSIG1, insulin-induced gene 1; ITGA, integrin subunit α; ITGB, integrin subunit β; MMP, matrix metallopeptidase; NSDHL, NAD(P) dependent steroid dehydrogenase-like; PANC-1, pancreatic cancer cell; PDAC, pancreatic ductal adenocarcinoma; PDGFβR, platelet-derived growth factor β receptor; PSC, pancreatic stellate cell; qPCR, quantitative PCR; shCTR, shRNA control; shITGA11, shRNA ITGA11; shRNA, short hairpin RNA; TIMP, TIMP metallopeptidase inhibitor

[1] Correspondence: Department of Biomaterials, Science, and Technology, TechMed Centre, Faculty of Science and Technology, Targeted Therapeutics Section, University of Twente, Zuidhorst 254, Enschede 7500 AE, The Netherlands. E-mail: j.prakash@utwente.nl

doi: 10.1096/fj.201802336R
This article includes supplemental data. Please visit *http://www.fasebj.org* to obtain this information.

stroma resulted in an aggressive tumor phenotype (10). Therefore, current strategies focus on modulating the activity of tumor stroma instead of completely depleting it to gain therapeutic benefits (8, 11–13). In human pancreatic cancer, the main progenitors of CAFs are human pancreatic stellate cells (hPSCs) (14). In the healthy pancreas, quiescent hPSCs have a cytoplasmic lipid storing capacity and are normally present in the connective tissue in low numbers, secreting only small amounts of ECM components (15). However, during malignancy, quiescent hPSCs get activated, lose their cytoplasmic lipid storing capacity, and secrete high amounts of ECM, which ultimately presents as a barrier for tumor drug penetration. In addition, activated hPSCs secrete various cytokines and growth factors, which stimulate tumor cells and other stromal cells, inducing tumor progression, metastasis, and drug resistance (16, 17). Activated hPSCs therefore present an attractive and promising cellular target for developing therapies to modulate tumor stroma.

Cellular interaction with the extracellular environment are mostly mediated by integrins, a known family of cell surface receptors, which have been recognized for their role in myofibroblast differentiation (18). In general, the integrin family consists of 24 different heterodimeric transmembrane receptors composed of different combinations of 18 different α-subunits and 8 different β-subunits (18). Because integrins build a physical connection with the inside and the outside of a cell, they are capable of conducting bidirectional signaling. Through this dynamic mechanism, integrins have the ability to control cellular cytoskeleton organization, thereby controlling crucial cellular functions, such as cell adhesion, migration, proliferation, survival, and differentiation (18, 19). Integrins are also known for their interaction with growth factors; for example, αv integrins can activate latent TGF-β1 (18, 20). Additionally, integrins interact with growth factor receptors *via* different mechanisms to regulate their signaling pathways (18, 21).

Integrins are therefore interesting target receptors to develop novel therapeutic strategies against tumor stroma. As collagens are the major ECM proteins in the tumor stroma, CAFs express one of the major collagen binding receptors (*i.e.*, integrin α11β1 (ITGA11). Integrin subtype α (ITGA) 11 has been shown to be overexpressed in the tumor stroma of head and neck squamous cell carcinoma, in which it positively correlated with the expression of CAF marker α–smooth muscle actin (α-SMA) (22). Additionally, ITGA11 was recognized for its role in inducing tumor cell growth and metastatic potential of small cell lung carcinoma cells (23). In this study, we investigated the expression and cellular localization of ITGA11 in human PDAC samples. Next, we studied the ITGA11 expression in activated hPSCs *in vitro* and demonstrated its role in regulating hPSC activation, differentiation, migration, and phenotypic changes using knockdown studies. Finally, we investigated the influence of ITGA11 knockdown on hPSC-mediated paracrine effect on tumor cells.

MATERIALS AND METHODS

Staining of human PDAC sections

Paraffin-embedded human PDAC sections and normal human pancreatic sections were obtained from Laboratory Pathology East Netherlands (LabPON; Hengelo, The Netherlands). Tissue sections were sliced, deparaffinized in xylene, and rehydrated in serially diluted alcohol solutions followed by demineralized water for 5 min, respectively. Antigen retrieval was performed in Tris EDTA buffer (pH 9.0) (Agilent Technologies, Santa Clara, CA, USA) by heat induction at 80°C. Endogenous peroxidase was blocked by incubation in 0.3% hydrogen peroxide (Thermo Fisher Scientific, Waltham, MA, USA) in methanol for 30 min.

After rinsing with Milli-Q water, the tissue sections were incubated overnight at 4°C with primary antibodies (**Table 1**) diluted in PBS. Control samples were incubated without primary antibodies in PBS overnight at 4°C. The slides were then incubated with the secondary and tertiary fluorescent antibody or horseradish peroxidase (HRP)-labeled antibody (Table 1) diluted in PBS supplemented with 5% normal human serum (Thermo Fisher Scientific), respectively, for 1 h at room temperature. Stainings performed with HRP-labeled antibodies were visualized using 3.3-diaminobenzidine tetrahydrochloride solution (Agilent Technologies) for 5–10 min, resulting in a brown color, and then counterstained with hematoxylin for 2 min. Subsequently, the tissue sections were dehydrated and mounted with VectaMount (Vector Laboratories, Burlingame, CA, USA). For staining with fluorescent antibodies, the slides were washed and mounted with Fluoroshield with DAPI (MilliporeSigma, Burlington, MA, USA) for staining of nuclei. All stained sections have been imaged using a Hamamatsu NanoZoomer Digital Slide Scanner 2.0HT (Hamamatsu Photonics, Hamamatsu, Japan), and visual scoring was performed on the scanned images.

TABLE 1. *Antibodies used for the staining of human PDAC and normal pancreas sections*

Antibody	Source	Dilution
Goat anti-ITGA11	R&D Systems (Minneapolis, MN, USA)	1:250
Mouse anti–α-SMA	MilliporeSigma	1:200
HRP-conjugated goat anti-rabbit IgG	Thermo Fisher Scientific	1:100
HRP-conjugated rabbit anti-goat IgG	Thermo Fisher Scientific	1:100
HRP-conjugated rabbit anti-mouse IgG	Thermo Fisher Scientific	1:100
Alexa Fluor 594–labeled donkey anti-goat	Thermo Fisher Scientific	1:100
Alexa Fluor 488−labeled donkey anti-mouse	Thermo Fisher Scientific	1:100

ITGA11 mRNA expression in the human cohort from the public database

We selected and downloaded 2 human pancreatic gene expression datasets from the Gene Expression Omnibus (GEO) database (National Center for Biotechnology Information, Bethesda, MD, USA: *https://www.ncbi.nlm.nih.gov/geo/*). The GSE28735 (24, 25) dataset comprises 41 normal and 41 pancreatic tumor tissues from 41 pancreatic tumor patients; GSE16515 (26) consists of 16 normal and 36 pancreatic tumor tissues. We used GEO2R to assess the expression of ITGA11 mRNA expression pancreatic tumor tissues *vs.* pancreatic nontumor tissues and plotted the gene expression levels.

Cell lines

Primary hPSCs (ScienCell Research Laboratories, Carlsbad, CA, USA), were cultured in complete Stellate Cell Medium [supplemented with 2% fetal bovine serum (FBS), 1% penicillin/streptomycin, and 1% Stellate Cell Growth Supplements] (ScienCell Research Laboratories). Pancreatic cancer cell line 1 (PANC-1) cancer cells were cultured in DMEM high glucose (4.5 g/L) with L-glutamine (GE Healthcare, Waukesha, WI, USA) supplemented with 10% FBS (Lonza, Basel, Switzerland) and 100 μg/ml penicillin/streptomycin (MilliporeSigma). The cells were maintained at 37°C in a humidified 5% CO_2 atmosphere.

Stable ITGA11 knockdown in hPSCs

To generate hPSCs with a stable knockdown of ITGA11 (shITGA11), primary hPSCs were transfected with either a scrambled short hairpin RNA (shRNA) control plasmid or shRNA ITGA11 plasmid using Lipofectamine 2000 (Thermo Fisher Scientific) as described by Bansal *et al.* (27). After 24 h of transfection with Lipofectamine, transfected cells were selected and cultured with 1 μg/ml of puromycin (Thermo Fisher Scientific).

Real-time quantitative PCR and RT^2 Profiler PCR Array

To evaluate the effect of ITGA11 knockdown on TGF-β–mediated hPSC activation, cells were seeded into a 12-well plate at a seeding density of 40,000 cells per well. The cells were starved for 24 h and activated with 5 ng/μl TGF-β or PANC-1 conditioned medium (CM). Twenty-four hours after activation, total RNA was isolated using the GenElute Mammalian Total RNA Miniprep Kit (MilliporeSigma). The amount of isolated RNA was measured by a NanoDrop ND-1000 Spectrophotometer (Thermo Fisher Scientific). Next, cDNA was synthesized with iScript cDNA Synthesis Kit (Bio-Rad, Hercules, CA, USA). Five nanograms cDNA was used for each real-time PCR reaction. Real-time PCR primers (**Table 2**) were purchased from (MilliporeSigma). Real-time PCR was performed using the 2× SensiMix Sybr and Fluorescein Kit (Bioline, London, United Kingdom) with a Bio-Rad CFX384 Real-Time PCR Detection System (Bio-Rad). For the Human Extracellular Matrix and Adhesion Molecules RT^2 Profiler PCR Array (Qiagen, Germantown, MD, USA), cDNA from 3 independent experiments was mixed and performed as described in the manufacturer's instructions, analyzed using the Data Analysis Center, and read with a Bio-Rad CFX384 Real-Time PCR Detection System.

Western blot analysis

Cells were prepared as previously described for real-time PCR analysis. Cells were lysed using 1× SDS lysis buffer. The cell lysis was centrifuged at 10,000 *g* for 10 min, and the supernatant was collected for Western blot analysis. In short, protein lysates and CM were loaded on 10% Tris-glycine gels (Thermo Fisher Scientific) and transferred onto PVDF membranes (Thermo Fisher Scientific). The membranes were incubated overnight at 4°C with the required primary antibody (**Table 3**) followed by incubation with species-specific HRP-conjugated secondary and tertiary antibody for 1 h at room temperature. HRP was detected with the Pierce ECL Plus Western Blotting Substrate Kit (Thermo Fisher Scientific) and exposed to FluorChem M System (Bio-Techne, Minneapolis, MN, USA). The protein levels were quantified by ImageJ software (National Institutes of Health, Bethesda, MD, USA).

F-actin staining

Cells were prepared as previously described for real-time quantitative PCR (qPCR). Subsequently, the cells were fixed in PBS

TABLE 2. *Sequences of forward and reverse primers used during real-time PCR*

	Primer, 5′–3′	
Gene	Forward	Reverse
RPS18	TGAGGTGGAACGTGTGATCA	CCTCTATGGGCCCGAATCTT
ITGA11	CAGCTCGCTGGAGAGATACG	TTACAGGACGTGTTCGCCTC
ACTA2 (*α-SMA*)	CCCCATCTATGAGGGCTATG	CAGTGGCCATCTCATTTTCA
ITGA11	CAGCTCGCTGGAGAGATACG	TTACAGGACGTGTTCGCCTC
PDGFβR	AGGCAAGCTGGTCAAGATCT	GCTGTTGAAGATGCTCTCCG
DESMIN	GCGGGTTTCGGCTCTAAGG	AGAAACTCCTGGTTCACCGC
COL1A1	GTACTGGATTGACCCCAACC	CGCCATACTCGAACTGGAAT
COL3A1	AAGAAGGCCCTGAAGCTGAT	GTGTTTCGTGCAACCATCCT
NSDHL	ATGCTATGGAGAGGACCGTG	CAGAAGGAGTCACAGGCTCA
CTGF	GTTTGGCCCAGACCCAACTA	GGCTCTGCTTCTCTAGCCTG
INSIG1	GGCAGCTTCCCAAGTATTCG	CTACCTCCTTTGGGCACTGA
IDI1	TTGGGCTGGATAAAACCCCT	GCAACATCCGGCATAACTGT
MMP2	AGGAGGAGAAGGCTGTGTTC	CTCCAGTTAAAGGCGGCATC
CXCR-4	GCGGTTACCATGGAGGGGAT	CCCATGACCAGGATGACCAAT

Col3a1, collagen type III α1 chain; RPS18, ribosomal protein S18.

containing 10% formaldehyde (MilliporeSigma) for 15 min. After permeabilization with 0.1 M Triton X-100 (MilliporeSigma) for 5 min, F-actin was stained with phalloidin (Thermo Fisher Scientific) at a concentration of 250 ng/ml for 30 min at room temperature. Next, cells were washed with PBS and imaged for phalloidin (excitation 540/emission 565) using an Evos FI Fluorescent Microscope (Thermo Fisher Scientific).

Immunocytochemistry

Cells were prepared as previously described for real-time qPCR. Next, cells were fixed and immunostained for α-SMA and collagen type I as described by Bansal *et al.* (28).

Cell proliferation assay

hPSCs were seeded at a density of 2500 cells per well into a 96-well plate, starved for 24 h, and activated with 5 ng/μl TGF-β or PANC-1 CM. Cell number was monitored every 24 h over a time period of 72 h. To measure the cell number, 10 μl of AlamarBlue Dye (Thermo Fisher Scientific) in 100 μl of hPSC growth medium was added per well. The fluorescent signal was measured after incubation for 4 h at 37°C using a Viktor Plate Reader (PerkinElmer, Waltham, MA, USA).

Three-dimensional collagen type I gel contraction assay

A collagen suspension consisting of 3.0 ml Collagen G1 (5 mg/ml; Matrix BioScience, Mörlenbach, Germany), 0.5 ml 10× M199 medium (MilliporeSigma), 85 μl 1 N NaOH (MilliporeSigma), and sterile water was mixed with 1.0 ml of cell suspension containing 200,000 shRNA control (shCTR) or shITGA11 hPSCs. Per well of a 24-well plate, 600 μl of collagen gel per cell was plated and allowed to form a gel for 1 h at 37°C. Once the collagen gel was formed, 1 ml of serum-free medium was added with or without TGF-β (5 ng/ml) or PANC-1 CM. Next, the gels were detached from the walls of the well plate with a 10-μl pipette tip. Representative images were made at 72 h using a digital camera. Measurements of collagen gel diameter were normalized with the diameter of the respective well and performed using ImageJ imaging software.

CM

To collect hPSC CM, shCTR and shITGA11 hPSCs were seeded into a 12-well plate at a seeding density of 40,000 cells per well. As previously described, cells were starved and activated with TGF-β or PANC-1 CM for 24 h. Next, the cells were washed 3 times with serum-free medium. After 48 h of incubation with serum-free medium, the medium was collected for use in CM experiments.

Wound healing assay

Cells were seeded into a 24-well plate at a seeding density of 50,000 cells per well. Cells were starved and TGF-β activated as previously described. To study migration, a scratch was made on the culture plate using a 200-μl pipette tip fixed in a custom-made holder. The cells were washed to remove all detached cells and incubated with fresh serum-free medium. Images were captured at 0 and 12 h with an Evos microscope. Images were analyzed by ImageJ software to calculate the area of the scratch and represented as the percentage of wound closure.

Transwell migration assay

PANC-1 cells were seeded at a density of 50,000 cells per well into the upper chamber of a 24-well, 8-μm Transwell insert (MilliporeSigma). The lower compartment of the Transwell insert was filled with CM from shITGA11 and shCTR hPSCs as chemoattractant. After 24 h, the cells were fixed with ice-cold methanol (Thermo Fisher Scientific) for 10 min and incubated with 0.1% crystal violet solution (MilliporeSigma) in 25% methanol for 10 min. After washing the cells with Milli-Q Water (MilliporeSigma), cells from the upper compartment were removed with a cotton swab. After drying the inserts, the migrated cells were imaged with a Nikon microscope (Eclipse E400; Nikon, Tokyo, Japan). The positively stained area per picture was analyzed by ImageJ software.

Transwell invasion assay

The upper and lower compartment of 8-μm BD Matrigel Invasion Chambers (BD Biosciences, San Jose, CA, USA) were filled with warm DMEM containing 0% FBS and rehydrated for 2 h at 37°C. Next the DMEM was removed from both compartments and PANC-1 cells were seeded at a density of 50,000 cells per well into the upper compartment of the invasion chamber. The lower compartment of the Transwell insert was filled with CM from shITGA11 and shCTR hPSCs as chemoattractant. After 48 h, the gel from the upper compartment was removed with a cotton swab. Next, the cells were fixed with ice-cold methanol for 10 min and incubated with 0.1% crystal violet solution in 25% methanol for 10 min and subsequently washed with Milli-Q water. After drying the inserts, the invaded cells were imaged with a Eclipse E400 Nikon microscope. The positively stained area per picture was analyzed by ImageJ software.

RESULTS

ITGA11 is specifically expressed by CAFs in human PDAC

Immunohistochemical analyses for ITGA11 expression in human PDAC sections showed clear and high

TABLE 3. *Primary and secondary antibodies used for Western blot*

Antibody	Source	Dilution
Goat-anti-ITGA11	R&D Systems (Minneapolis, MN, USA)	1:250
Mouse anti–α-SMA	MilliporeSigma	1:200
Mouse monoclonal anti–β-actin	MilliporeSigma	1:10,000
HRP-conjugated goat anti-rabbit IgG	Thermo Fisher Scientific	1:2000
HRP-conjugated rabbit anti-goat IgG	Thermo Fisher Scientific	1:2000
HRP-conjugated rabbit anti-mouse IgG	Thermo Fisher Scientific	1:1000

expression levels in the tumor stroma, whereas no expression was observed in the tumor epithelial cells. In addition, ITGA11 was completely absent in normal human pancreatic tissues (**Fig. 1*A***). We have previously shown that ITGA11 is absent in healthy human and mouse liver and lungs, whereas it is overexpressed in fibroblasts during fibrotic diseases of kidney, liver, and lungs (27). In this study, we also examined other human organs, such as kidneys, liver, skin, and small intestine, and found no expression of ITGA11 (Supplemental Fig. S1). Visual scoring (n = 6 patients) was based on the percentage of stroma positive area for ITGA11 staining as high, moderate, and low for >65, 35–65, and <35%, respectively. In total, 66.7% of stained tumors showed a moderate to low expression of ITGA11 in the tumor stroma, whereas 33.3% showed high stromal expression levels. Additionally, we found that ITGA11 was expressed by CAFs, as demonstrated with colocalization immunofluorescent double staining with the CAF marker α-SMA (Fig. 1*B*). The double

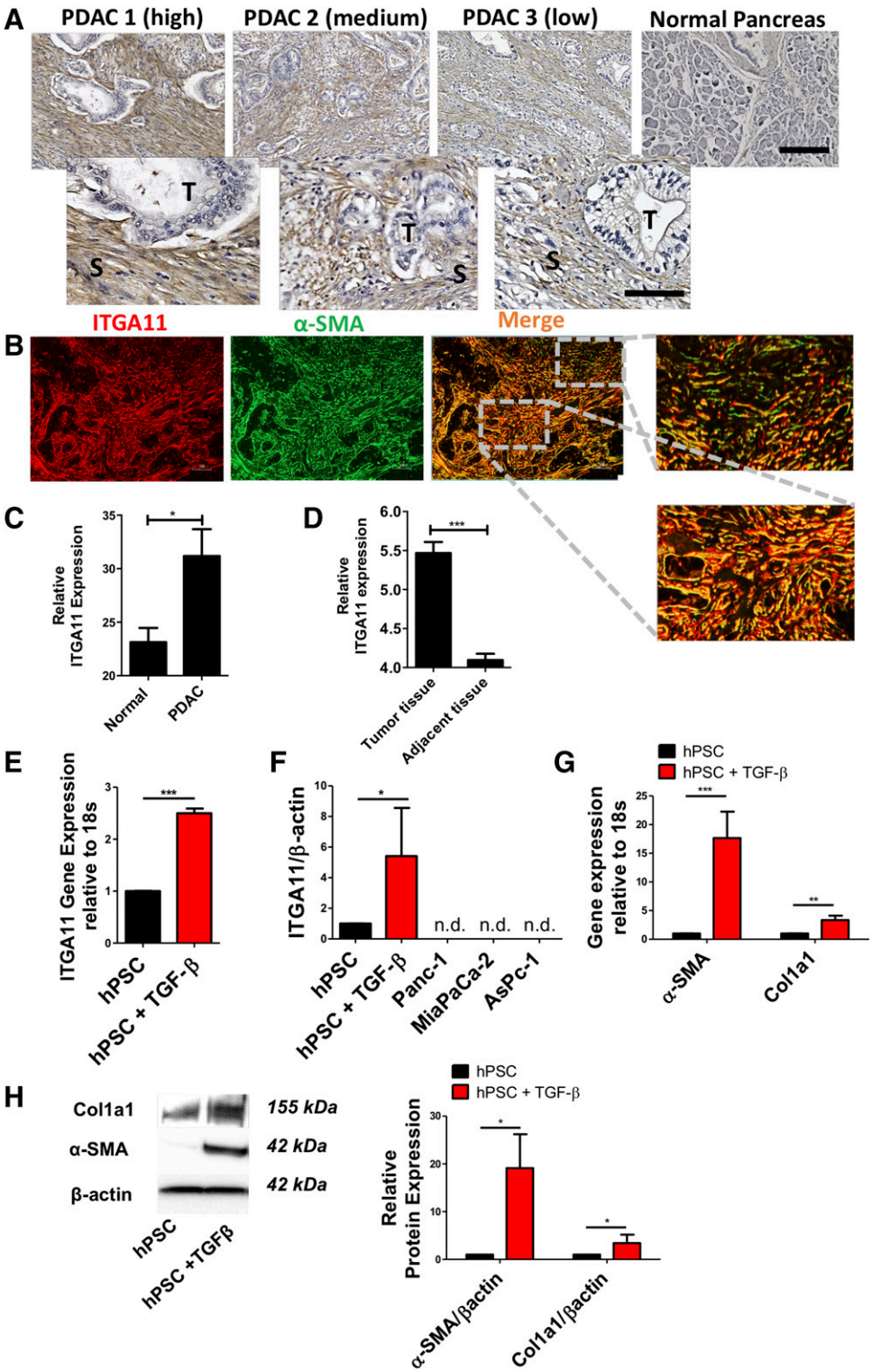

Figure 1. ITGA11 expression in human pancreatic tumor tissue and activated PSCs. *A*) Staining of human PDAC and normal pancreas for ITGA11. Scale bar, 250 μm. High-magnification images are shown as subsets. S, stroma; T, tumor nest. Scale bar, 100 μm. High, moderate, and low staining indicate the >65, 33–65, and <33% positive area for the ITGA11 staining, respectively. *B*) Colocalization of ITGA11 with α-SMA. *C*) Transcriptome analysis showing ITGA11 expression in 16 normal human pancreatic tissues and 36 human PDAC tissues. *D*) Transcriptome analysis performed on 45 human patients comparing ITGA11 expression in pancreatic tumor *vs.* adjacent nontumor tissue within the same patient. *E*, *F*) Gene expression (*E*) and protein expression (*F*) of ITGA11 in TGF-β–activated and nonactivated hPSCs and 3 different tumor cell lines. *G*, *H*) Gene expression (*G*) and protein expression (*H*) of α-SMA and Col1a1 in TGF-β–activated and nonactivated hPSCs. N.d. not detected. Data represent the mean ± SEM for ≥3 independent experiments. Statistical analysis was performed by a 2-tailed, unpaired Student's *t* test. $^{*}P < 0.05$, $^{**}P < 0.01$, $^{***}P < 0.001$.

immunofluorescence staining data showed that 80% of α-SMA–positive cells were also ITGA11-positive and 20% of α-SMA–positive cells were ITGA11 negative, whereas only 5% of ITGA11-positive cells were negative for α-SMA (Fig. 1*B*). Transcriptome analysis on public data showed that ITGA11 is found to be significantly induced in the tumor tissue compared with normal pancreatic tissue in 45 patients (Fig. 1*C*). In addition, a significant induction of ITGA11 expression levels was found in human PDAC compared with adjacent non-tumor tissues (Fig. 1*D*).

TGF-β induces ITGA11 expression in hPSCs

To determine whether ITGA11 expression is specifically induced in primary human activated hPSCs, we compared the gene and protein expression of ITGA11 in TGF-β–activated and nonactivated control hPSCs. We found that ITGA11, on both gene and protein levels, was expressed in low levels in nonactivated hPSCs, whereas its expression levels were induced in TGF-β–activated cells (Fig. 1*E*). Additionally, no expression of ITGA11 was found in the human pancreatic cancer cell lines PANC-1, MiaPaCa-2, and AsPc-1 (Fig. 1*F*). Furthermore, the induction of ITGA11 was in line with hPSC activation markers collagen type I α1 chain (Col1a1) and α-SMA, as shown at gene and protein levels (Fig. 1*G*, *H*).

Knockdown of ITGA11 inhibits TGF-β– and PANC-1 CM–mediated differentiation of hPSCs

To demonstrate the role for ITGA11 in hPSC activation, we stably knocked down ITGA11 in hPSCs using shRNA plasmid and evaluated the effect of the ITGA11 knockdown on the hPSC phenotype and TGF-β–mediated activation and differentiation. The knockdown of ITGA11 was confirmed using real-time qPCR and Western blot analysis, showing a reduction of about 50% at the mRNA level and about 85% at the protein level in ITGA11 knockdown (shITGA11) hPSC compared with the control (shCTR) hPSCs (**Fig. 2*A*, *B***). ITGA11 knockdown resulted in a drastic phenotypic change, leading to cellular hypertrophy compared with shCTR hPSCs (Fig. 2*C*).

Upon activation with TGF-β, both shCTR and shITGA11 hPSCs showed only a slight induction in ITGA11 levels (Fig. 2*D*). Of note, surprisingly, we found that the induction of ITGA11 and α-SMA protein levels with TGF-β in plasmid-treated hPSCs (either shCTR or shITGA11) was less than those with normal hPSCs (Fig. 2*D vs.* Fig. 1*E*–*H*), which might be attributed to higher passage numbers, which was unavoidable to achieve stable transfection. Interestingly, TGF-β–mediated induction of α-SMA in shITGA11 hPSCs was significantly attenuated compared with shCTR hPSCs (Fig. 2*D*). As shown previously by Fernando *et al.* (29), CM of PANC-1 tumor cells contains a mixture of different cytokines, such as IL-8, IGF binding protein 1, osteoprotegrin, VEGF, angiogenin, IGF binding protein 2, placental growth factor, and granulocyte-macrophage colony-stimulating factor. We evaluated whether knockdown of ITGA11 in hPSCs attenuated not only TGF-β–induced differentiation but also PANC-1 CM–induced differentiation of hPSCs. We investigated the influence of PANC-1 CM on ITGA11 expression and PANC-1 CM–induced activation of hPSCs and shITGA11 hPSCs. Unlike TGF-β treatment, treatment of hPSCs with PANC-1 CM did not induce ITGA11 levels in either shITGA11 or shCTR hPSCs (Fig. 2*E*). The protein expression of α-SMA was induced in shCTR hPSCs activated with PANC-1 CM, whereas these inductions were attenuated in shITGA11 hPSCs. Immunostaining showed the same trend for the protein expression of Col1a1 and α-SMA, both in TGF-β and PANC-1 CM activated shITGA11 hPSCs (Fig. 2*F*, *G*).

Additionally, we examined the effect of ITGA11 knockdown on CAF markers and found that ITGA11 knockdown significantly down-regulated the gene expression of CAF markers, such as platelet-derived growth factor β receptor (PDGFβR), desmin, collagen type III α1 chain (COL3A1), NAD(P) dependent steroid dehydrogenase-like (NSDHL), insulin-induced gene 1 (INSIG1), isopentenyl-diphosphate Δ-isomerase 1 (IDI1), and C-X-C chemokine receptor type 4 (CXCR-4) (**Fig. 3**). Upon activation with TGF-β, shITGA11 hPSCs showed an attenuated expression in the CAF markers PDGFβR, desmin, NSDHL, INSIG1, IDI1, and CXCR-4 as compared with shCTR hPSCs (Fig. 3*A*), indicating that these genes are regulated by ITGA11. When these cells were activated with PANC-1 CM, the CAF markers α-SMA, PDGFβR, desmin, INSIG1, and CXCR-4 showed an attenuated expression in shITGA11 as compared with shCTR hPSCs (Fig. 3*B*). It needs to be noted that among these markers only PDGFβR was significantly induced with PANC-1 CM.

We further analyzed shCTR and shITGA11 hPSCs with and without TGF-β–mediated activation for the mRNA gene expression profiling of 84 ECM and adhesion proteins using a human profiler gene array. Genes down-regulated after the knockdown of ITGA11 included various receptors responsible for the adhesion to immune cells [selectin E, integrin subunit β (ITGB) 2, selectin P, integrin subunit α (ITGA)L, selectin L, ITGAM, ITGA4]; laminin receptors (ITGA7, ITGB4); collagen receptors (ITGA8); Arg-Gly-Asp receptors (ITGA3); ECM molecules (COL7A1, COL11A1, COL12A1, COL15A1, COL16A1, ECM protein 1, laminin subunit α (LAMA)1, LAMA3, vitronectin); MMPs (matrix metallopeptidases) and TIMP metallopeptidase inhibitors (TIMPs) (MMP8, MMP9, MMP10, MMP11, MMP12, MMP13, TIMP3, and ADAM metallopeptidase with thrombospondin type 1 motif 8); cell adhesion molecules (contactin 1, cadherin 1, catenin Δ2, thrombospondin 2, C-type lectin domain family 3 member B, neural cell adhesion molecule 1); and a protein involved in ECM production (hyaluronan synthase 1) (Supplemental Table S1).

Furthermore, we identified TGF-β–induced genes that are regulated by ITGA11. We found several genes whose expression was less induced in shITGA11 hPSCs compared with shCTR hPSCs after activation with TGF-β or PANC-1 CM (**Tables 4 and 5**). The extended lists are

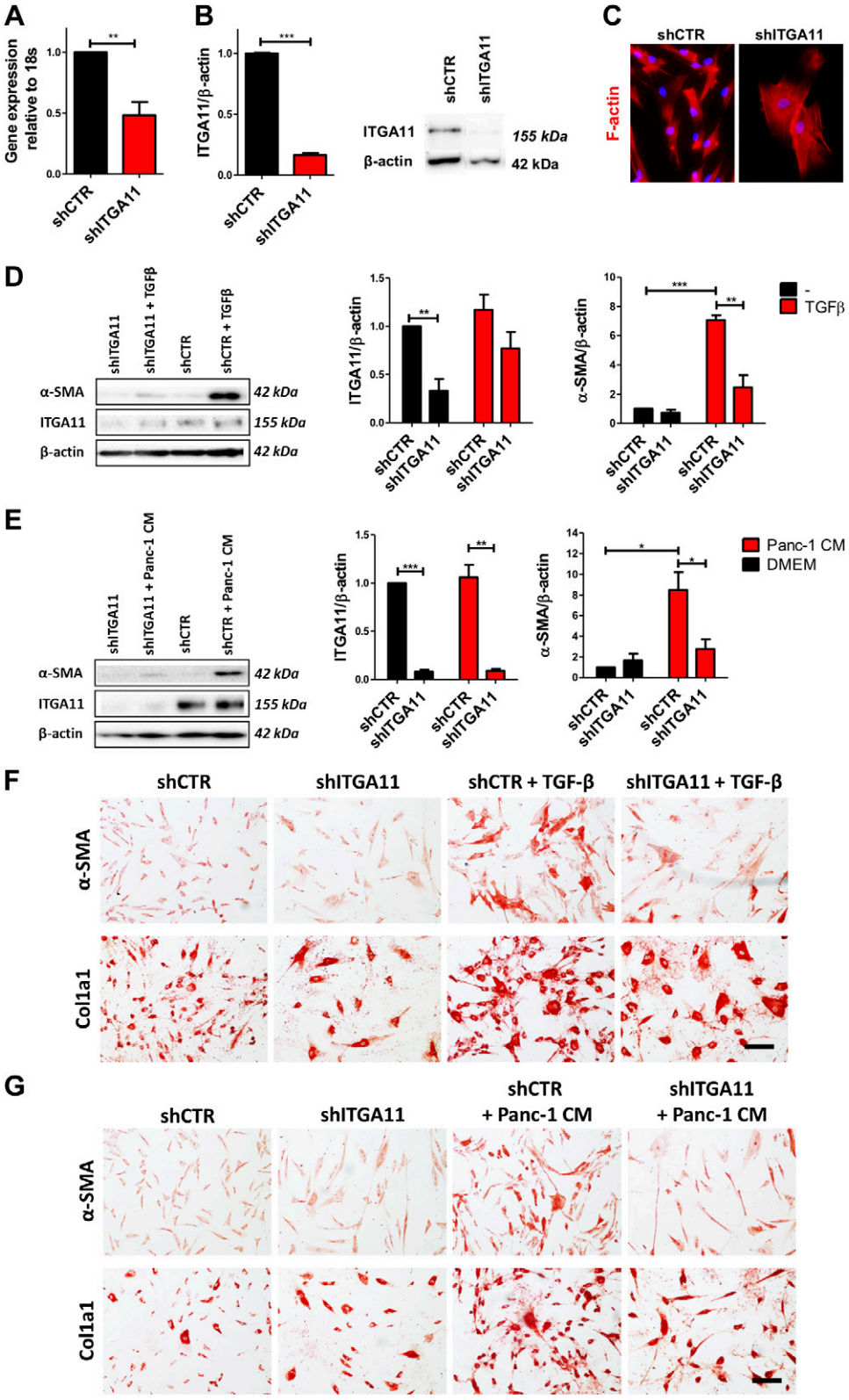

Figure 2. Knockdown of ITGA11 inhibits TGF-β– and PANC-1 CM–mediated activation of PSCs. *A*, *B*) Real-time qPCR (*A*) and Western blot (*B*) showing shRNA–mediated knockdown of ITGA11. *C*) F-actin staining of shCTR compared with shITGA11 hPSCs. Scale bar, 50 μm. *D*) Western blot for ITGA11 and α-SMA of shCTR and shITGA11 hPSCs with and without TGF-β activation. *E*) Western blot for ITGA11 and α-SMA of shCTR and shITGA11 hPSCs with and without PANC-1 CM activation. *F*) Immunostaining for α-SMA and Col1a1 of shCTR and shITGA11 hPSCs with and without TGF-β activation. Scale bar, 200 μm. *G*) Immunostaining for α-SMA and Col1a1 of shCTR and shITGA11 hPSCs with and without PANC-1 CM activation. Scale bar, 200 μm. Data represent the mean ± SEM for ≥3 independent experiments. Statistical analysis was performed by a 2-tailed, unpaired Student's *t* test. $^{*}P < 0.05$, $^{**}P < 0.01$, $^{***}P < 0.001$.

presented in Supplemental Tables S2 and S3. These included cell adhesion molecules (THBS1, SPP1); collagen receptors (ITGA2); Arg-Gly-Asp receptors (ITGB3, ITGA5); growth factors (CTGF); ECM molecules (TNC, FN1, COL8A1, COL11A1, TGFBI); MMPs and TIMPs (TIMP1, MMP1, MMP3); and protein involved in ECM production (SPARC).

Knockdown of ITGA11 attenuates TGF-β– and PANC-1 CM–induced hPSC function

We further investigated whether ITGA11 regulates the functions of hPSCs, including migration and contraction. hPSCs are known for their ability to migrate to the tumor site and differentiate into CAFs with

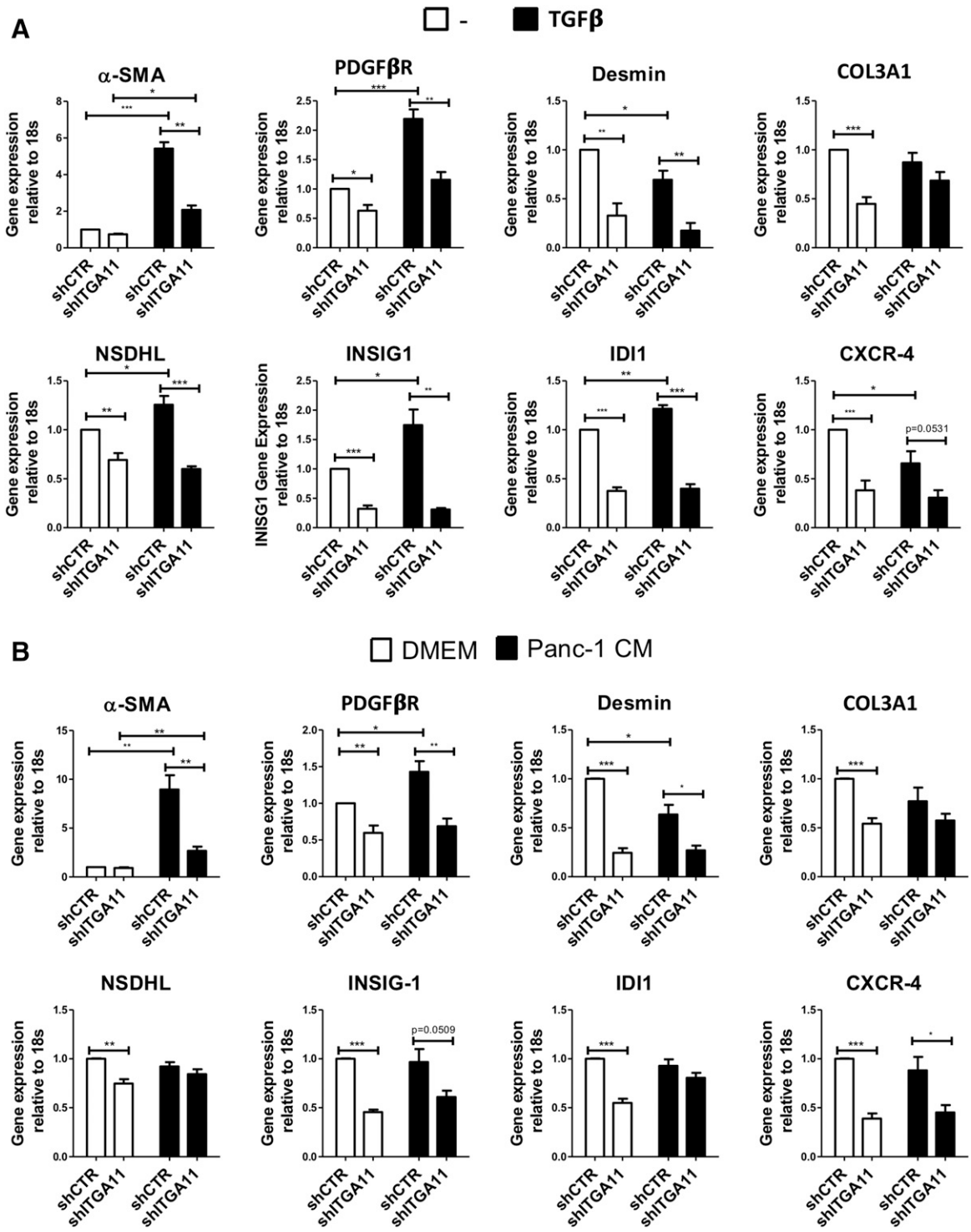

Figure 3. Knockdown of ITGA11 inhibits TGF-β– and PANC-1 CM–mediated differentiation of hPSCs. *A*) Real-time qPCR of hPSCs activated with TGF-β for the CAF markers α-SMA, PDGFβR, desmin, COL3A1, NSDHL, INSIG1, IDI1, and CXCR-4. *B*) Real-time qPCR of hPSCs activated with PANC-1 CM for the CAF markers α-SMA, PDGFβR, desmin, COL3A1, NSDHL, INSIG1, IDI1, and CXCR-4. Data represent the mean ± SEM for at ≥3 independent experiments. Statistical analysis was performed by a 2-tailed, unpaired Student's *t* test. $*P < 0.05$, $**P < 0.01$, $***P < 0.001$.

high contractile properties and support metastasis (30). Although nonactivated hPSCs do not have the ability to contract, hPSCs activated with TGF-β or PANC-1 CM acquire a contractile phenotype. In comparison with shCTR hPSCs, shITGA11 hPSCs showed significantly poor contractile ability (**Fig. 4*A, B***). Furthermore, cell migration (with and without TGF-β induction) within 12 h was attenuated in shITGA11 hPSCs as compared with shCTR hPSCs (Fig. 4*C*). In contrast to TGF-β activation, PANC-1 CM did not show induction of migration of shCTR hPSC, yet ITGA11 knockdown reduced the migration of hPSCs (Fig. 4*D*). These data indicate that ITGA11 can regulate the activation of hPSCs by controlling more pathways than only TGF-β.

TABLE 4. *List of top genes that were least up-regulated after the treatment with TGF-β in shITGA11 hPSCs compared with shCTR hPSCs*

Gene	RefSeq	Description	Fold change		Δ Change
			shCTR + TGF-β	shITGA11 + TGF-β	
THBS1	NM_003246	Thrombospondin 1	14.26	3.32	10.94
CTGF	NM_001901	Connective tissue growth factor	6.22	2.81	3.41
TNC	NM_002160	Tenascin C	7.65	5.92	1.73
TIMP1	NM_003254	TIMP metallopeptidase inhibitor 1	2.49	1.06	1.43
MMP3	NM_002422	Matrix metallopeptidase 3	2.41	1.43	0.98
SPP1	NM_001251830	Secreted phosphoprotein 1	2.71	1.82	0.89
FN1	NM_212474	Fibronectin 1	2.28	1.73	0.55
COL8A1	NM_001850	Collagen type VIII α1 chain	2.47	1.96	0.51
SPARC	NM_003118	Secreted protein acidic and cysteine rich	2.16	1.86	0.3
TGFBI	NM_000358	TGF-β induced	2.25	1.96	0.29

Fold regulation was calculated with the respective nonactivated controls (shCTR or shITGA11 hPSCs). The data were obtained with the Human Extracellular Matrix and Adhesion Molecules RT^2 Profiler PCR Array and analyzed using the Data Analysis Center. The extended list is incorporated in the Supplemental Data. RefSeq, reference sequence.

Knockdown of ITGA11 in pancreatic stellate cells inhibits paracrine effects on tumor cells

We first examined whether hPSC CM collected after activation with either TGF-β or PANC-1 CM induced migration and invasion of PANC-1 cells, which was due to epithelial mesenchymal transition in PANC-1 cells, as shown in Supplemental Fig. S2. After confirming the direct effects of ITGA11 knockdown on hPSC activation, we investigated whether ITGA11 knockdown can inhibit hPSC-mediated paracrine effects on tumor cell migration and invasion. To evaluate this, we collected CM from nonactivated and TGF-β– or PANC-1 CM–activated shCTR and shITGA11 hPSCs and put on PANC-1 cells.

We found that PANC-1 cells incubated with CM obtained from shITGA11 hPSCs had a reduced ability to migrate and invade compared with the CM from shCTR hPSCs (**Fig. 5**). These data demonstrate that ITGA11 in pancreatic stellate cells (PSCs) plays a critical role in controlling TGF-β– or PANC-1 CM–activated PSC secretome, which acts as a stimulant for tumor cell migration and invasion.

DISCUSSION

The present study introduces the collagen type I–binding transmembrane receptor ITGA11 as a regulator for the PSC differentiation and protumorigenic functions in pancreatic cancer. ITGA11 was shown to be substantially expressed in the stroma of human PDAC and colocalized with the major CAF marker α-SMA. Strikingly, the knockdown of ITGA11 in hPSCs inhibited their differentiation, migration, and contractility. A gene profiler array showed that many ECM and adhesion molecules were down-regulated in hPSCs after ITGA11 knockdown. Moreover, our data revealed that the knockdown of ITGA11 attenuated hPSC-mediated paracrine effects on PANC-1 tumor cells. These findings suggest ITAG11 as a potential therapeutic target for inhibiting ECM production and paracrine effect of PSCs.

The pancreatic tumor stroma is well known as one of the hallmarks of PDAC. CAFs, the most abundant stromal cells, promote PDAC progression by producing high amounts of ECM and secreting various cytokines and growth factors, which in turn stimulate tumor

TABLE 5. *List of top genes that were least up-regulated after the treatment with PANC-1 CM in shITGA11 hPSCs compared with shCTR hPSCs*

Gene	RefSeq	Description	Fold change		Δ Change
			shCTR + PANC-1 CM	shITGA11+ PANC-1 CM	
TNC	NM_002160	Tenascin C	9.94	3.56	6.38
MMP1	NM_001145938	Matrix metallopeptidase 1	5.77	2.17	3.6
MMP3	NM_002422	Matrix metallopeptidase 3	4.38	1.83	2.55
ITGA2	NM_002203	Integrin subunit α2	5.02	2.54	2.48
THBS1	NM_003246	Thrombospondin 1	5.76	4.1	1.66
FN1	NM_212474	Fibronectin 1	3.03	1.81	1.22
ITGB3	NM_000212	Integrin subunit β3	2.68	1.5	1.18
COL11A1	NM_001854	Collagen type XI α1 chain	3.54	2.69	0.85
ITGA5	NM_002205	Integrin subunit α5	2.19	1.79	0.4

Fold regulation was calculated with the respective nonactivated controls (shCTR or shITGA11 hPSCs). The data were obtained with the Human Extracellular Matrix and Adhesion Molecules RT^2 Profiler PCR Array and analyzed using the Data Analysis Center. The extended list is incorporated in the Supplemental Data. RefSeq, reference sequence.

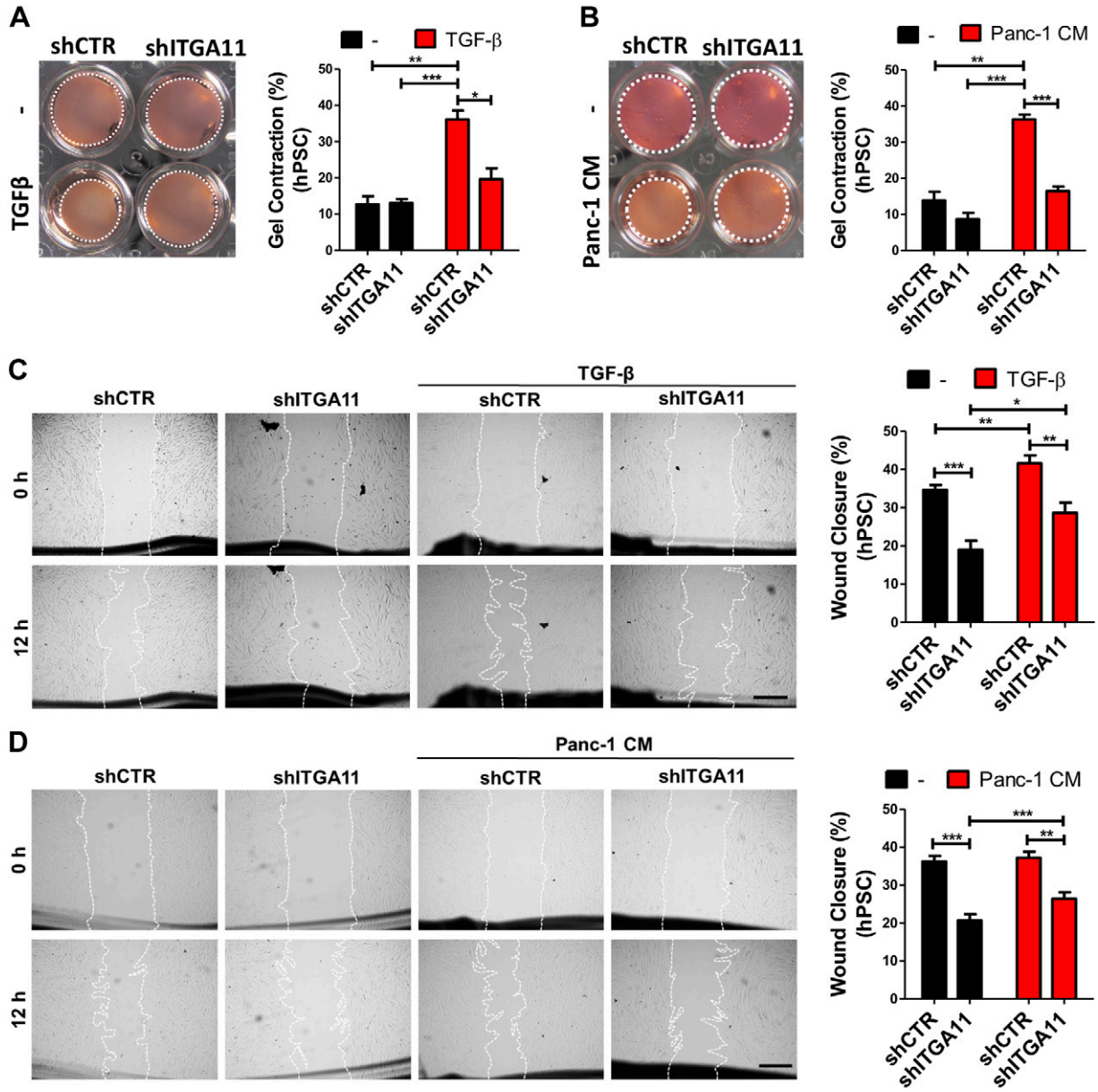

Figure 4. Knockdown of ITGA11 attenuates TGF-β–induced hPSC function. *A*) Representative images and quantification of collagen gel contraction of shCTR and shITGA11 hPSCs with and without TGF-β activation. *B*) Representative images and quantification of collagen gel contraction by shCTR and shITGA11 hPSCs with and without PANC-1 CM activation. *C*) Representative microscopic images and quantification showing the migration of shCTR and shITGA11 hPSCs with and without TGF-β activation. *D*) Representative microscopic images and quantification showing the migration of shCTR and shITGA11 hPSCs with and without PANC-1 CM activation. Scale bars, 500 μm. Data represent the mean ± SEM for at ≥3 independent experiments. Statistical analysis was performed by a 2-tailed, unpaired Student's *t* test. $^{*}P < 0.05$, $^{**}P < 0.01$, $^{***}P < 0.001$.

growth, angiogenesis, invasion, and metastasis (5–7, 31). hPSCs are regarded as the main precursors of CAFs in the pancreatic tumor stroma (16), and in response to TGF-β, they acquire a CAF-like myofibroblast phenotype, as we and others have previously shown (32–34). Recent studies have demonstrated that PSCs can differentiate into 2 different CAF subtypes: myofibroblast-like CAFs (driven by TGF-β) and inflammatory CAFs (driven by IL-1–induced JAK/signal transducer and activator of transcription pathway) (35, 36). Therefore, modulating the tumor stroma through therapeutic strategies that aim to inhibit the activation of hPSCs into CAFs is a rational approach to gain therapeutic benefits for the treatment of PDAC (13). ECM transmembrane receptors of the integrin family allow cells to attach, migrate, and proliferate. Some integrin receptors are strongly up-regulated in CAFs, which by themselves produce high amounts of ECM, including collagens (18). Integrin targeting in myofibroblasts has been shown to inhibit fibrosis in multiple organs, such as liver, lung, and kidney (18, 27, 37, 38). Targeting to ITGA11 will be selective to a fibrotic disease or PDAC due to its absence or very low expression in other organs, as shown in our previous study in liver and lungs (27) and this study (kidneys, liver, skin, and small intestine).

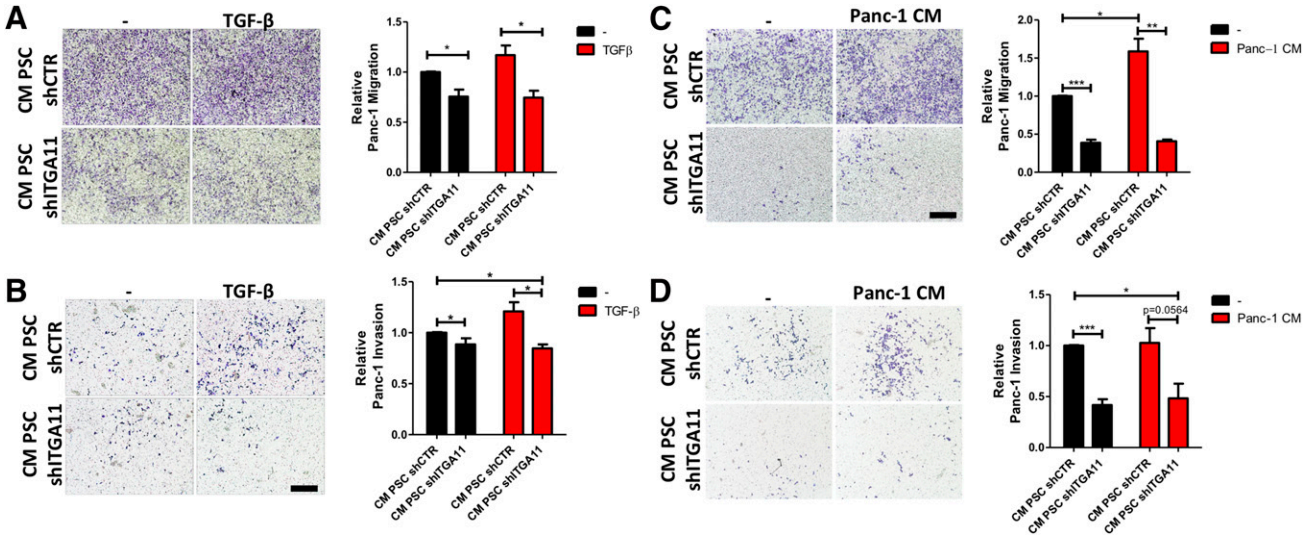

Figure 5. CM from hPSCs with shITGA11 inhibit paracrine effects on PANC-1 migration and invasion. Representative images and quantification of PANC-1 tumor cell migration (*A*, *C*) and invasion (*B*, *D*) after incubation with CM obtained from shCTR and shITGA11 hPSCs after TGF-β (*A*, *B*) or PANC-1 CM (*C*, *D*) activation. For migration studies, PANC-1 cells were incubated with the CM for 24 h, whereas for invasion assay, they were incubated with CM for 48 h. Scale bars, 400 μm. Statistical analysis was performed by a 2-tailed, unpaired Student's *t* test. $*P < 0.05$, $**P < 0.01$, $***P < 0.001$.

With transcriptome analysis, we show that ITGA11 expression is induced in human PDAC compared with healthy human pancreas. Furthermore, when comparing nontumoral pancreatic tissues to human tumor tissues within 45 patients, ITGA11 shows significantly higher expression in the tumoral part of the pancreas. In the present study, we show for the first time that ITGA11 is highly up-regulated in the tumor stroma of human PDAC. Coimmunostaining of ITGA11 with α-SMA showed that ITGA11 was almost exclusively expressed on CAFs within these tissues, with 80% of α-SMA–positive cells being ITGA11-positive and only 20% of α-SMA–positive cells being ITGA11 negative. Interestingly, no expression of ITGA11 was found in healthy pancreatic tissue, suggesting it as a specific therapeutic target.

We found that quiescent hPSCs had an extremely low expression of ITGA11, whereas activation with TGF-β resulted in a significant up-regulation of ITGA11, which correlated with the significant up-regulation of the main CAF markers, α-SMA and Col1a1. The induction of ITGA11 can be attributed to the TGF-β–mediated regulation of ITGA11 in a Smad-specificity protein 1 (Smad-Sp1)–dependent manner, which was previously demonstrated by Lu *et al.* (39). Stable knockdown of ITGA11 in hPSCs significantly attenuated the TGF-β– and PANC-1 CM–mediated differentiation of hPSCs and ECM production, as shown with the CAF-related markers α-SMA and COL1A1 (Figs. 2 and 3). In addition, ITGA11 knockdown significantly reduced the TGF-β– and PANC-1 CM–induced expression of PDGFβR, desmin, NSDHL, IDI1, INSIG1, MMP-2, and CXCR-4. These markers were previously found to be induced in activated PSCs by transcriptome analysis (8, 40). Of high significance is the down-regulation of ECM proteins (*e.g.*, collagens limiting chemotherapeutic activity by blocking drug delivery) (41, 42). In addition, the gene profiler array for ECM and cell adhesion molecules revealed genes that were controlled by ITGA11, as shown by the knockdown of ITGA11. Among them, selectin, connectin, and TIMP3 were the top down-regulated genes. Furthermore, we also revealed TGF-β– and PANC-1 CM–induced genes regulated by ITGA11 in hPSCs, and among them, thrombospondin and CTGF, known to decrease the tumor response to gemcitabine (43) and TNC, correlating with the differentiation of pancreatic cancer (44), were the most reduced ones (Tables 4 and 5).

We further studied whether ITGA11 controls the phenotype and activation of PSCs. Interestingly, ITGA11 knockdown resulted in a loss of cell contractility or migration with and without TGF-β or PANC-1 CM–mediated activation of hPSCs. Overall, these data demonstrate that ITGA11 is crucial for the maintenance of the phenotypic features and activation of hPSCs.

Because hPSCs crosstalk with tumor cells and other stromal cells in the tumor microenvironment, we examined the effect of ITGA11 on the paracrine effects hPSCs exert on cancer cells. It has previously been demonstrated that hPSCs can induce tumor-promoting paracrine effects by secreting mutagenic factors such as growth factors and cytokines to induce tumor progression, invasion, and metastasis (5, 16). In this study, we found that after the treatment with hPSC CM, PANC-1 cells went under epithelial mesenchymal transition, as shown in Supplemental Fig. S2, which led to the increased migration and invasion of these cells. Interestingly, we found that CM from shITGA11 hPSCs, with and without activation with TGF-β or PANC-1 CM, showed an attenuated migration and invasion of PANC-1 tumor cells compared with shCTR hPSCs. This further demonstrates the role of ITGA11 in regulating the tumor-promoting phenotype of hPSCs.

In summary, the present study for the first time demonstrates the expression and role of ITGA11 in PSCs in pancreatic tumor stroma. ITGA11 was specifically and

strongly expressed in the tumor stroma colocalized with CAFs. Furthermore, we show ITGA11 as a crucial target in maintenance of the phenotype and activation and differentiation of hPSCs. Nonetheless, our knockdown studies demonstrated a direct regulatory effect of ITGA11 on the transcriptome and secretome of activated hPSCs, thereby controls their paracrine function. Altogether, ITGA11 is a promising therapeutic target for developing new therapeutics to inhibit the hPSC-mediated crosstalk in the tumor microenvironment. FJ

ACKNOWLEDGMENTS

This study was supported by the Swedish Research Council (Project 2011-5389). J.P. is a founder and stakeholder of ScarTec Therapeutics (Enschede). The remaining authors declare no conflicts of interest.

AUTHOR CONTRIBUTIONS

J. Schnittert and J. Prakash designed the research; J. Schnittert and D. F. Mardhian performed the experiments; J. Schnittert and J. Prakash analyzed data and wrote the manuscript; R. Bansal analyzed data and refined the manuscript; A. Östman contributed by discussing the research results; and J. van Baarlen contributed human tumor tissue samples.

REFERENCES

1. Siegel, R. L., Miller, K. D., and Jemal, A. (2017) Cancer statistics, 2017. *CA Cancer J. Clin.* **67**, 7–30
2. Conroy, T., Desseigne, F., Ychou, M., Bouché, O., Guimbaud, R., Bécouarn, Y., Adenis, A., Raoul, J. L., Gourgou-Bourgade, S., de la Fouchardière, C., Bennouna, J., Bachet, J. B., Khemissa-Akouz, F., Péré-Vergé, D., Delbaldo, C., Assenat, E., Chauffert, B., Michel, P., Montoto-Grillot, C., and Ducreux, M.; Groupe Tumeurs Digestives of Unicancer; PRODIGE Intergroup. (2011) FOLFIRINOX versus gemcitabine for metastatic pancreatic cancer. *N. Engl. J. Med.* **364**, 1817–1825
3. Von Hoff, D. D., Ervin, T., Arena, F. P., Chiorean, E. G., Infante, J., Moore, M., Seay, T., Tjulandin, S. A., Ma, W. W., Saleh, M. N., Harris, M., Reni, M., Dowden, S., Laheru, D., Bahary, N., Ramanathan, R. K., Tabernero, J., Hidalgo, M., Goldstein, D., Van Cutsem, E., Wei, X., Iglesias, J., and Renschler, M. F. (2013) Increased survival in pancreatic cancer with nab-paclitaxel plus gemcitabine. *N. Engl. J. Med.* **369**, 1691–1703
4. Xie, D., and Xie, K. (2015) Pancreatic cancer stromal biology and therapy. *Genes Dis.* **2**, 133–143
5. Hwang, R. F., Moore, T., Arumugam, T., Ramachandran, V., Amos, K. D., Rivera, A., Ji, B., Evans, D. B., and Logsdon, C. D. (2008) Cancer-associated stromal fibroblasts promote pancreatic tumor progression. *Cancer Res.* **68**, 918–926
6. Apte, M. V., and Wilson, J. S. (2012) Dangerous liaisons: pancreatic stellate cells and pancreatic cancer cells. *J. Gastroenterol. Hepatol.* **27** (Suppl 2), 69–74
7. Vonlaufen, A., Joshi, S., Qu, C., Phillips, P. A., Xu, Z., Parker, N. R., Toi, C. S., Pirola, R. C., Wilson, J. S., Goldstein, D., and Apte, M. V. (2008) Pancreatic stellate cells: partners in crime with pancreatic cancer cells. *Cancer Res.* **68**, 2085–2093
8. Sherman, M. H., Yu, R. T., Engle, D. D., Ding, N., Atkins, A. R., Tiriac, H., Collisson, E. A., Connor, F., Van Dyke, T., Kozlov, S., Martin, P., Tseng, T. W., Dawson, D. W., Donahue, T. R., Masamune, A., Shimosegawa, T., Apte, M. V., Wilson, J. S., Ng, B., Lau, S. L., Gunton, J. E., Wahl, G. M., Hunter, T., Drebin, J. A., O'Dwyer, P. J., Liddle, C., Tuveson, D. A., Downes, M., and Evans, R. M. (2014) Vitamin D receptor-mediated stromal reprogramming suppresses pancreatitis and enhances pancreatic cancer therapy. *Cell* **159**, 80–93
9. Provenzano, P. P., Cuevas, C., Chang, A. E., Goel, V. K., Von Hoff, D. D., and Hingorani, S. R. (2012) Enzymatic targeting of the stroma ablates physical barriers to treatment of pancreatic ductal adenocarcinoma. *Cancer Cell* **21**, 418–429
10. Özdemir, B. C., Pentcheva-Hoang, T., Carstens, J. L., Zheng, X., Wu, C. C., Simpson, T. R., Laklai, H., Sugimoto, H., Kahlert, C., Novitskiy, S. V., De Jesus-Acosta, A., Sharma, P., Heidari, P., Mahmood, U., Chin, L., Moses, H. L., Weaver, V. M., Maitra, A., Allison, J. P., LeBleu, V. S., and Kalluri, R. (2014) Depletion of carcinoma-associated fibroblasts and fibrosis induces immunosuppression and accelerates pancreas cancer with reduced survival. *Cancer Cell* **25**, 719–734; erratum: 28, 831–833
11. Shields, M. A., Dangi-Garimella, S., Redig, A. J., and Munshi, H. G. (2012) Biochemical role of the collagen-rich tumour microenvironment in pancreatic cancer progression. *Biochem. J.* **441**, 541–552
12. Kuninty, P. R., Schnittert, J., Storm, G., and Prakash, J. (2016) MicroRNA targeting to modulate tumor microenvironment. *Front. Oncol.* **6**, 3
13. Prakash, J. (2016) Cancer-associated fibroblasts: perspectives in cancer therapy. *Trends Cancer* **2**, 277–279
14. Bachem, M. G., Schneider, E., Gross, H., Weidenbach, H., Schmid, R. M., Menke, A., Siech, M., Beger, H., Grünert, A., and Adler, G. (1998) Identification, culture, and characterization of pancreatic stellate cells in rats and humans. *Gastroenterology* **115**, 421–432
15. Habisch, H., Zhou, S., Siech, M., and Bachem, M. G. (2010) Interaction of stellate cells with pancreatic carcinoma cells. *Cancers (Basel)* **2**, 1661–1682
16. Apte, M. V., Wilson, J. S., Lugea, A., and Pandol, S. J. (2013) A starring role for stellate cells in the pancreatic cancer microenvironment. *Gastroenterology* **144**, 1210–1219
17. Bachem, M. G., Schünemann, M., Ramadani, M., Siech, M., Beger, H., Buck, A., Zhou, S., Schmid-Kotsas, A., and Adler, G. (2005) Pancreatic carcinoma cells induce fibrosis by stimulating proliferation and matrix synthesis of stellate cells. *Gastroenterology* **128**, 907–921
18. Schnittert, J., Bansal, R., Storm, G., and Prakash, J. (2018) Integrins in wound healing, fibrosis and tumor stroma: high potential targets for therapeutics and drug delivery. *Adv. Drug Deliv. Rev.* **129**, 37–53
19. Seguin, L., Desgrosellier, J. S., Weis, S. M., and Cheresh, D. A. (2015) Integrins and cancer: regulators of cancer stemness, metastasis, and drug resistance. *Trends Cell Biol.* **25**, 234–240
20. Conroy, K. P., Kitto, L. J., and Henderson, N. C. (2016) αv integrins: key regulators of tissue fibrosis. *Cell Tissue Res.* **365**, 511–519
21. Ivaska, J., and Heino, J. (2011) Cooperation between integrins and growth factor receptors in signaling and endocytosis. *Annu. Rev. Cell Dev. Biol.* **27**, 291–320
22. Parajuli, H., Teh, M. T., Abrahamsen, S., Christoffersen, I., Neppelberg, E., Lybak, S., Osman, T., Johannessen, A. C., Gullberg, D., Skarstein, K., and Costea, D. E. (2017) Integrin α11 is overexpressed by tumour stroma of head and neck squamous cell carcinoma and correlates positively with alpha smooth muscle actin expression. *J. Oral Pathol Med.* **46**, 267–275
23. Navab, R., Strumpf, D., To, C., Pasko, E., Kim, K. S., Park, C. J., Hai, J., Liu, J., Jonkman, J., Barczyk, M., Bandarchi, B., Wang, Y. H., Venkat, K., Ibrahimov, E., Pham, N. A., Ng, C., Radulovich, N., Zhu, C. Q., Pintilie, M., Wang, D., Lu, A., Jurisica, I., Walker, G. C., Gullberg, D., and Tsao, M. S. (2016) Integrin α11β1 regulates cancer stromal stiffness and promotes tumorigenicity and metastasis in non-small cell lung cancer. *Oncogene* **35**, 1899–1908
24. Zhang, G., He, P., Tan, H., Budhu, A., Gaedcke, J., Ghadimi, B. M., Ried, T., Yfantis, H. G., Lee, D. H., Maitra, A., Hanna, N., Alexander, H. R., and Hussain, S. P. (2013) Integration of metabolomics and transcriptomics revealed a fatty acid network exerting growth inhibitory effects in human pancreatic cancer. *Clin. Cancer Res.* **19**, 4983–4993
25. Zhang, G., Schetter, A., He, P., Funamizu, N., Gaedcke, J., Ghadimi, B. M., Ried, T., Hassan, R., Yfantis, H. G., Lee, D. H., Lacy, C., Maitra, A., Hanna, N., Alexander, H. R., and Hussain, S. P. (2012) DPEP1 inhibits tumor cell invasiveness, enhances chemosensitivity and predicts clinical outcome in pancreatic ductal adenocarcinoma. *PLoS One* **7**, e31507
26. Badea, L., Herlea, V., Dima, S. O., Dumitrascu, T., and Popescu, I. (2008) Combined gene expression analysis of whole-tissue and microdissected pancreatic ductal adenocarcinoma identifies genes specifically overexpressed in tumor epithelia. *Hepatogastroenterology* **55**, 2016–2027

27. Bansal, R., Nakagawa, S., Yazdani, S., van Baarlen, J., Venkatesh, A., Koh, A. P., Song, W. M., Goossens, N., Watanabe, H., Beasley, M. B., Powell, C. A., Storm, G., Kaminski, N., van Goor, H., Friedman, S. L., Hoshida, Y., and Prakash, J. (2017) Integrin alpha 11 in the regulation of the myofibroblast phenotype: implications for fibrotic diseases. *Exp. Mol. Med.* **49**, e396
28. Bansal, R., Post, E., Proost, J. H., de Jager-Krikken, A., Poelstra, K., and Prakash, J. (2011) PEGylation improves pharmacokinetic profile, liver uptake and efficacy of Interferon gamma in liver fibrosis. *J. Control. Release* **154**, 233–240
29. Fernando, R. I., Castillo, M. D., Litzinger, M., Hamilton, D. H., and Palena, C. (2011) IL-8 signaling plays a critical role in the epithelial-mesenchymal transition of human carcinoma cells. *Cancer Res.* **71**, 5296–5306
30. Karagiannis, G. S., Poutahidis, T., Erdman, S. E., Kirsch, R., Riddell, R. H., and Diamandis, E. P. (2012) Cancer-associated fibroblasts drive the progression of metastasis through both paracrine and mechanical pressure on cancer tissue. *Mol. Cancer Res.* **10**, 1403–1418
31. Yazdani, S., Bansal, R., and Prakash, J. (2017) Drug targeting to myofibroblasts: implications for fibrosis and cancer. *Adv. Drug Deliv. Rev.* **121**, 101–116
32. Kuninty, P. R., Bojmar, L., Tjomsland, V., Larsson, M., Storm, G., Östman, A., Sandström, P., and Prakash, J. (2016) MicroRNA-199a and -214 as potential therapeutic targets in pancreatic stellate cells in pancreatic tumor. *Oncotarget* **7**, 16396–16408
33. Costa-Silva, B., Aiello, N. M., Ocean, A. J., Singh, S., Zhang, H., Thakur, B. K., Becker, A., Hoshino, A., Mark, M. T., Molina, H., Xiang, J., Zhang, T., Theilen, T. M., García-Santos, G., Williams, C., Ararso, Y., Huang, Y., Rodrigues, G., Shen, T. L., Labori, K. J., Lothe, I. M., Kure, E. H., Hernandez, J., Doussot, A., Ebbesen, S. H., Grandgenett, P. M., Hollingsworth, M. A., Jain, M., Mallya, K., Batra, S. K., Jarnagin, W. R., Schwartz, R. E., Matei, I., Peinado, H., Stanger, B. Z., Bromberg, J., and Lyden, D. (2015) Pancreatic cancer exosomes initiate pre-metastatic niche formation in the liver. *Nat. Cell Biol.* **17**, 816–826
34. Sarper, M., Cortes, E., Lieberthal, T. J., and Del Río Hernández, A. (2016) ATRA modulates mechanical activation of TGF-β by pancreatic stellate cells. *Sci. Rep.* **6**, 27639
35. Öhlund, D., Handly-Santana, A., Biffi, G., Elyada, E., Almeida, A. S., Ponz-Sarvise, M., Corbo, V., Oni, T. E., Hearn, S. A., Lee, E. J., Chio, I. I., Hwang, C. I., Tiriac, H., Baker, L. A., Engle, D. D., Feig, C., Kultti, A., Egeblad, M., Fearon, D. T., Crawford, J. M., Clevers, H., Park, Y., and Tuveson, D. A. (2017) Distinct populations of inflammatory fibroblasts and myofibroblasts in pancreatic cancer. *J. Exp. Med.* **214**, 579–596
36. Biffi, G., Oni, T. E., Spielman, B., Hao, Y., Elyada, E., Park, Y., Preall, J., and Tuveson, D. A. (2018) IL1-induced JAK/STAT signaling is antagonized by TGFβ to shape CAF heterogeneity in pancreatic ductal adenocarcinoma. [E-pub ahead of print] *Cancer Discov.* 10.1158/2159-8290.CD-18-0710
37. Reed, N. I., Jo, H., Chen, C., Tsujino, K., Arnold, T. D., DeGrado, W. F., and Sheppard, D. (2015) The αvβ1 integrin plays a critical in vivo role in tissue fibrosis. *Sci. Transl. Med.* **7**, 288ra79
38. Henderson, N. C., Arnold, T. D., Katamura, Y., Giacomini, M. M., Rodriguez, J. D., McCarty, J. H., Pellicoro, A., Raschperger, E., Betsholtz, C., Ruminski, P. G., Griggs, D. W., Prinsen, M. J., Maher, J. J., Iredale, J. P., Lacy-Hulbert, A., Adams, R. H., and Sheppard, D. (2013) Targeting of αv integrin identifies a core molecular pathway that regulates fibrosis in several organs. *Nat. Med.* **19**, 1617–1624
39. Lu, N., Carracedo, S., Ranta, J., Heuchel, R., Soininen, R., and Gullberg, D. (2010) The human alpha11 integrin promoter drives fibroblast-restricted expression in vivo and is regulated by TGF-beta1 in a Smad- and Sp1-dependent manner. *Matrix Biol.* **29**, 166–176
40. Kalluri, R. (2016) The biology and function of fibroblasts in cancer. *Nat. Rev. Cancer* **16**, 582–598
41. Minchinton, A. I., and Tannock, I. F. (2006) Drug penetration in solid tumours. *Nat. Rev. Cancer* **6**, 583–592
42. Netti, P. A., Berk, D. A., Swartz, M. A., Grodzinsky, A. J., and Jain, R. K. (2000) Role of extracellular matrix assembly in interstitial transport in solid tumors. *Cancer Res.* **60**, 2497–2503
43. Neesse, A., Frese, K. K., Bapiro, T. E., Nakagawa, T., Sternlicht, M. D., Seeley, T. W., Pilarsky, C., Jodrell, D. I., Spong, S. M., and Tuveson, D. A. (2013) CTGF antagonism with mAb FG-3019 enhances chemotherapy response without increasing drug delivery in murine ductal pancreas cancer. *Proc. Natl. Acad. Sci. USA* **110**, 12325–12330
44. Juuti, A., Nordling, S., Louhimo, J., Lundin, J., and Haglund, C. (2004) Tenascin C expression is upregulated in pancreatic cancer and correlates with differentiation. *J. Clin. Pathol.* **57**, 1151–1155

Received for publication October 31, 2018.
Accepted for publication January 28, 2019.